# Arsenic removal from water using N,N-diethylethanolammonium chloride based DES-functionalized CNTs: (NARX) neural network approach

Seef Saadi Fiyadh, Mohammed Abdulhakim AlSaadi, Mohamed Khalid AlOmar, Sabah Saadi Fayaed and Ahmed El-Shafie

## ABSTRACT

In this paper, the deep eutectic solvent-functionalized carbon nanotube was used for arsenic removal from water solution. The adsorbent used was characterized using Raman spectroscopy, Fourier transform infrared (FTIR) and zeta potential. The effect of the parameters (adsorbent dosage, pH, initial concentration and contact time) was studied to find the optimum conditions for maximum adsorption capacity of the functionalized carbon nanotube. The pseudo-second-order, the pseudo-first-order and intraparticle diffusion kinetic models were applied to identify the adsorption rate and mechanism, the pseudo-second-order model best described the adsorption kinetics of the system. The non-linear autoregressive network with exogenous inputs (NARX) neural network strategy was used for the modelling and predicting of the adsorption capacity of functionalized carbon nanotube. Different indicators were used to determine the efficiency and accuracy of the NARX neural network model which were mean square error (MSE), root mean square error (RMSE), relative root mean square error (RRMSE) and mean absolute percentage error (MAPE). The sensitivity study of the used parameters in the experimental work was completed. Comparison of the NARX model results with the experimental data confirmed that the NARX model was able to predict the arsenic removal from water.

**Key words** | arsenic ions, carbon nanotubes, deep eutectic solvents, NARX neural network, water treatment

**Seef Saadi Fiyadh**
**Mohammed Abdulhakim AlSaadi**
(corresponding author)
Nanotechnology and Catalysis Research Centre (NANOCAT), IPS Building,
University of Malaya,
50603 Kuala Lumpur,
Malaysia
E-mail: *mdsd68j@gmail.com*

**Mohammed Abdulhakim AlSaadi**
**Mohamed Khalid AlOmar**
University of Malaya Centre for Ionic Liquids,
University of Malaya,
Kuala Lumpur 50603,
Malaysia

**Mohammed Abdulhakim AlSaadi**
National Chair of Materials Science and Metallurgy,
University of Nizwz, Sultanate of Oman,
Nizwa,
Oman

**Mohamed Khalid AlOmar**
**Ahmed El-Shafie**
Civil Engineering Department, Faculty of Engineering,
Komar University of Science and Technology,
Sulaymaniyah,
Iraq

**Sabah Saadi Fayaed**
Department of Civil Engineering,
University of Malaya,
Kuala Lumpur 50603,
Malaysia

## LIST OF ABBREVIATIONS

| | |
|---|---|
| ANN | Artificial neural network |
| CNT | Carbon nanotube |
| DAC | N,N-diethylethanolammonium chloride |
| DES | Deep eutectic solvent |
| FTIR | Fourier transform infrared |
| Gly | Glycerol |
| HBA | Hydrogen bond acceptor |
| HBD | Hydrogen bond donor |
| MAPE | Mean absolute percentage error |
| MSE | Mean square error |
| MWCNT | Multi-wall carbon nanotube |
| NARX | Non-linear autoregressive network with exogenous inputs |
| P-CNT | Pristine carbon nanotube |
| $Q_c$ | Adsorption capacity |
| RE | Relative error |
| RMSE | Root mean square error |
| RRMSE | Relative root mean square error |

doi: 10.2166/aqua.2018.107

## INTRODUCTION

The presence of heavy metal ions in water is considered as a major problem due to their non-biodegradability, toxicity and human health complications. Arsenic is one of the heavy metals known as a carcinogenic material to humans. It can be found in polluted groundwater as a result of industrial waste discharge, rock weathering, pesticides and arsenical herbicides use for agricultural purposes (Xia *et al.* 2014). The exposure and consumption of arsenic polluted drinking water causes numerous health problems in several countries such as Bangladesh (Wasserman *et al.* 2004), Bengal (Mazumder *et al.* 1997) and China (Wang *et al.* 2007). Due to the serious health problems related to arsenic in drinking water, the World Health Organization determined the maximum allowable arsenic in drinking water as 10 μg/L (Smith *et al.* 2002). Several hundreds of mg/L of arsenic concentration are available in groundwater. Consequently, millions of people are affected due to the high contamination of drinking water with arsenic (Argos *et al.* 2010). Many chemical, biological and physical processes have been utilized for heavy metal treatment such as precipitation, ion-exchange, reverse osmosis, biosorption, filtration and adsorption (Ding *et al.* 2014; Ahmadi *et al.* 2015; Cho *et al.* 2015; Luo *et al.* 2015). Adsorption is the most suitable technique due to its cost effectiveness, feasible operation and high removal efficiency (Kamble *et al.* 2007; Kocabaş-Ataklı & Yürüm 2013; Hu *et al.* 2015; Ramos *et al.* 2016). In addition, this method has the ability to remove small concentrations of heavy metals from a large amount of water solutions. The effectiveness of adsorption mainly depends on the selection of appropriate process conditions such as the mass of sorbent, pH, system temperature and the process duration (Lourie & Gjengedal 2011). Various studies have been conducted using different materials like clay minerals, biomaterials and activated carbon for heavy metal ions removal from water (Chen & Wu 2004; Gupta *et al.* 2006; Oubagaranadin & Murthy 2010). However, the use of traditional adsorbents has common drawbacks such as small adsorption capacity and low adsorption efficiency (Rao *et al.* 2007). Consequently, highly efficient adsorbents are necessary to remove the arsenic ions from water solution. Therefore, the development of new adsorbents has become the major interest of researchers in water treatment technology.

Nanoparticles are one of the most popular adsorbents for several pollutants, owing to their features, such as catalytic potential, small size, large surface area and high reactivity (Ali 2012). Carbon nanotubes (CNTs) possess different properties from other materials used, which make them suitable for many applications in electronics, water treatment, optics, nanotechnology and other material science fields (Atieh *et al.* 2011). However, carbon nanotubes have some limitations ascribed to various flaws in solubility, difficulty in manipulation and aggregation. Hence, surface modification of carbon nanotubes has magnificent affinity by interfacing with other compounds (Thostenson *et al.* 2001; Sun *et al.* 2002). The CNTs' surface charge can be enhanced by the oxidative functionalization. However, this method requires the use of strong acids, which is not environmentally friendly. Therefore, the need for an environmentally friendly modification technique is crucial for the widespread application of CNTs (Martinez *et al.* 2003; Hayyan *et al.* 2015).

Deep eutectic solvents (DESs) are identified as the liquid combination formed by the complexation of hydrogen bond acceptors (HBAs) and hydrogen bond donors (HBDs) (Abbott *et al.* 2004; Gorke *et al.* 2008; Zhang *et al.* 2012). DESs are new green solvents with many advantages as compared to the ionic liquids (ILs) (Xu *et al.* 2015). The prime advantages of DESs over conventional ILs are the diversity of physical properties and different molar ratios, ease of synthesis and cheaper price of raw materials. The DESs are synthesized from two or more inexpensive materials, consisting of non-flammable and usually non-toxic components which are able to connect together via hydrogen bonding (Paiva *et al.* 2014). The components mixture has a lower melting point than the individual compounds (Abbott *et al.* 2004).

Recently, DESs have been reported in many applications; examples include the uses of ChCl-based DES as a functional additive for starch-based plastics (Leroy *et al.* 2012), the synthesis of zeolite analogues (Cooper *et al.* 2004), mediums for the deposition of specific metals in electro and electroless plating of metals (Abbott *et al.* 2007, 2008), and most recently, in nanotechnology applications (Abo-Hamad *et al.* 2015).

In general, the adsorption process is considered complicated for heavy metal removal due to the influence of

many variables such as contact time, adsorbent dosage, pH and initial heavy metal concentration. The conventional linear method for modelling this kind of process is hectic. On the other hand, the artificial neural networks (ANNs) modelling technique, which is known as a robust black-box modelling tool, is capable of transforming a given dataset into its target outputs. The ANN capability to generalize and learn the behaviour of any non-linear and complex process makes it a powerful tool. ANNs consist of a massive parallel numerical architecture which can solve complicated problems by the assistance of highly connected neurons organized in layers. Recently, the ANNs technique has been used for various engineering applications (Fayaed *et al.* 2013; Fiyadh *et al.* 2017). Some studies suggest the NARX neural network is suitable for non-linear systems modelling (McAvoy & Werbos 1992; Çoruh *et al.* 2014).

The objective of this study was to synthesize a DES by mixing glycerol (Gly) with N,N-diethylethanolammonium chloride, for CNTs functionalization. Subsequently, the DES-functionalized CNTs were utilized as an adsorbent for arsenic removal from water. Furthermore, the NARX neural network was used for modelling and establishing the relationship that exists between the operational variables.

## MATERIALS AND METHODOLOGY

This section describes the materials used in DES synthesis, multi-wall carbon nanotubes (MWCNTs) functionalization by DES and the functionalized CNTs characterization. The materials used in the experimental work were hydrochloric acid (36.5–38%), Glycerol (Gly), potassium permanganate ($KMnO_4$), MWCNTs with specification of L 5 μm × D 6–9 nm, >95% carbon, and sodium hydroxide pellets and were all provided by Sigma Aldrich. Arsenic standard solution of 1,000 mg/L and N,N-diethylethanolammonium chloride (DAC) > 99% purity were provided by Merck, Germany.

The DES synthesis was performed by mixing DAC and Gly at a molar ratio of 2:1 HBD:salt (AlOmar *et al.* 2016b), at 80 °C temperature for 3 hours until the DES became homogenous. The produced DES is referred to as D in this study. The prepared DES was kept in a tightly controlled environment to avoid the effect of humidity.

The first step of the functionalization was to dry the pristine MWCNTs (P-CNTs) at 100 °C overnight. Then, 200 mg of the dried P-CNTs was mixed with 7 mL of $KMnO_4$ and sonicated for 2 h at 65 °C to produce K-CNTs. The functionalization by D-DES was achieved by mixing 7 mL of the prepared D-DES with 200 mg of K-CNTs and sonicating them at 65 °C for 3 h to produce DK-CNTs. After that, the filtration process was performed by washing the functionalized CNTs using distilled water and filtering with a PTFE 0.45 μm membrane until the pH of the filtered water reached neutral. Later, the washed functionalized CNTs were dried overnight at 100 °C before being used for the removal.

Raman spectroscopy, Fourier transform infrared (FTIR) and zeta potential were used for the characterization of P-CNTs, K-CNTs and DK-CNTs adsorbent. The Raman shift was obtained to identify the degree of functionalization using a Renishaw System 2000 Raman Spectrometer. The FTIR was used to identify the surface chemical modification of the adsorbent using FTIR spectroscopy via a PerkinElmer® FTIR spectrometer, USA, with a range of 400–4,000 wave number and four times repetition. Zetasizer (Malvern, UK) was used to recognize the adsorbent partial surface charge by measuring the zeta potential. The surface area of the adsorbent was measured using a fully Automated Gas Sorption System (micromeritics ASAP2020, TRISTAR II 3020 Kr®, USA) (AlOmar *et al.* 2016a).

### Adsorption experiments

The functionalized DK-CNTs adsorbent was used for arsenic removal from water solution. The experiments were conducted with various dosages of DK-CNTs adsorbent (20 to 40 mg), arsenic concentration (1 to 5 mg/L), and with different pH values (3 to 8). The pH of the solution was controlled using NaOH and HCl. A volume of 50 ml of contaminated water was poured into 250-mL flasks, the flasks were shaken at 180 rpm using a mechanical system at room temperature. The number of samples prepared in this study was 156. The arsenic concentrations were tested at different time intervals to study the

adsorption equilibrium time using inductively coupled plasma (ICP) with an OES OPTIMA 7000DV PerkinElmer®, USA.

## NARX neural network modelling and evaluation indicators

An artificial neural network is a tool that can generate and capture the linear and non-linear relationship between dependent and independent variables (Agami *et al.* 2009). The NARX neural network is a dynamic network which contains various layers with a back-propagation connection (Chen *et al.* 1990). The NARX neural network is well known for its high speed of convergence as well as its high degree of generalization.

The NARX neural network was trained and used in this study for modelling the adsorption capacity of the DK-CNTs adsorbent. NARX is a recurrent dynamic network, it consists of feedback connections with several layers. The iterative training process is used in the NARX models whereby the weights and biases are adjusted iteratively to improve the performance of the model at each step. When including the information from the exogenous inputs, the NARX models get an extra degree of freedom compared with other networks. This improves the accuracy of the models and decreases the number of parameters required for the model. The NARX outputs during the training are presented in Equation (1).

$$y(t) = f(u(t-n_u), \ldots .u(t-1), u(t), y(t-n_y), \ldots .y(t-1)) \quad (1)$$

where:

$f$ is the non-linear function.
$u_{(t)}$ is the network inputs at time $t$.
$y_{(t)}$ is the network outputs at time $t$.
$n_u$ and $n_y$ are the order of inputs and outputs.

During the training, the outputs of the network regress on the target of the actual values as long as they are accessible. Within the training process, the values of the actual target are fed back to the network. This basically results in a better learning and training, and the network acts as feed-forward network which is always steady. The resulting system is known as a NARX network, when the $f$ approach is used with multi-layer perception (Chen *et al.* 1990). In this paper, two-layers of NARX were used (presented in Figure 1) for the prediction of the adsorption capacity ($Q_c$) of the DK-CNTs. The input layer of the network consists of four inputs (time, adsorbent dosage, pH and initial concentration) and there is one output layer ($Q_c$). In Figure 1, $b_h$ is the network bias, $w_{ij}$ is the network weight and $z$ is the delay element.

Various indicators were employed in this study for the evaluation of the NARX model using the predicted and actual results to check the reliability of the NARX model. These indicators are the relative root mean square error (RRMSE), mean square error (MSE), root mean square error (RMSE), mean absolute percentage error (MAPE) and relative error (RE).

$$RRMSE = \left[\frac{1}{n}\sum_{t=1}^{n}\left(\frac{D_{a(t)} - D_{f(t)}}{D_{a(t)}}\right)^2\right]^{1/2} \quad (2)$$

$$MSE = \frac{1}{n}\sum_{i=1}^{n}\left(D_{a(t)} - D_{f(t)}\right)^2 \quad (3)$$

$$RMSE = \left[\frac{1}{n}\sum_{t=1}^{n}\left(D_{a(t)} - D_{f(t)}\right)^2\right]^{1/2} \quad (4)$$

$$MAPE = \frac{1}{n}\sum_{t=1}^{n}\left|\frac{\left(D_{a(t)} - D_{f(t)}\right)}{D_{a(t)}}\right| \times 100 \quad (5)$$

$$RE = \frac{D_{a(t)} - D_{f(t)}}{D_{a(t)}} \times 100 \quad (6)$$

where:

$D_{f(t)}$ = the predicted value.
$D_{a(t)}$ = the actual value.

The RRMSE, MSE, RMSE, MAPE and RE are the indicators that were used for evaluating the model performance. The aim of using different indicators is to confirm the accuracy of the model. All the indicators are based on the obtained results by comparing the error between the actual and predicted results.

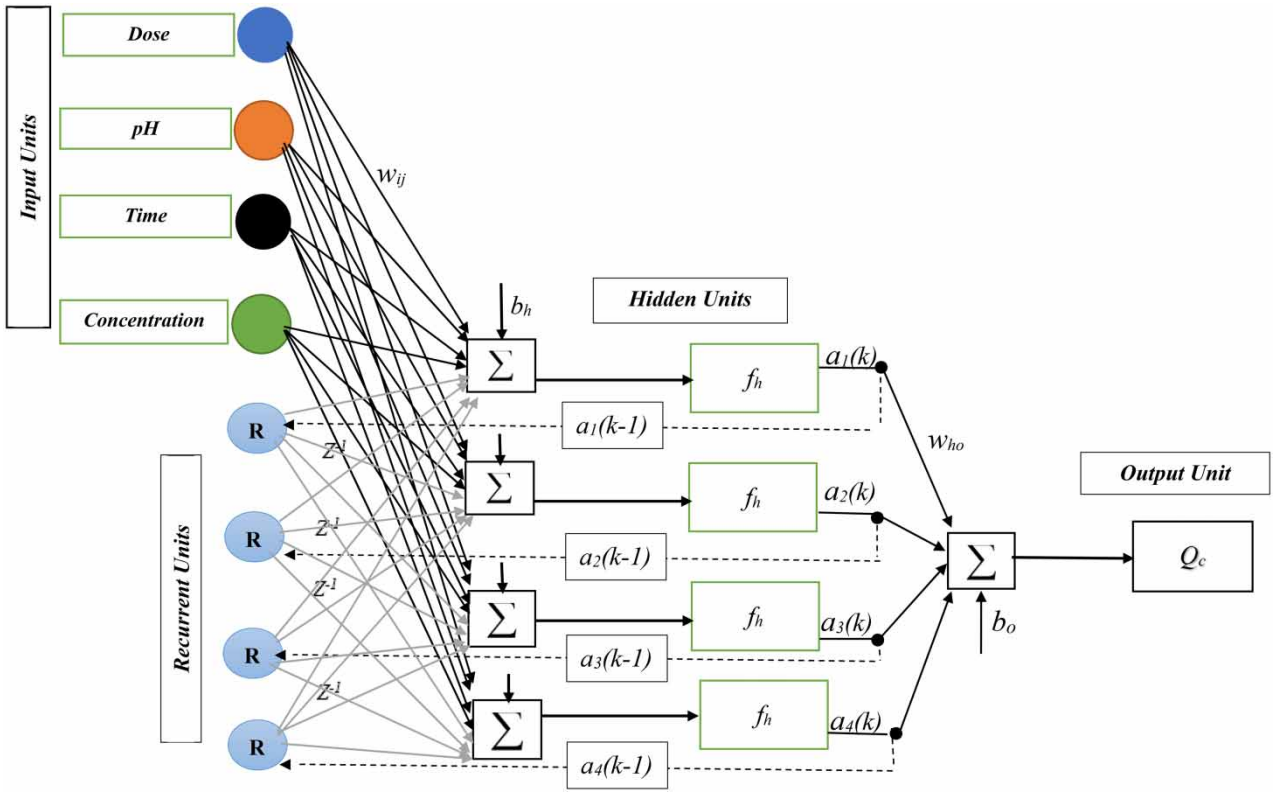


**Figure 1** | The NARX neural network structure.

## RESULTS AND DISCUSSION

In this study, a new adsorbent was prepared (DK-CNTs) and used for arsenic removal from water. The NARX neural network was used for the modelling of the adsorption capacity and different indicators were utilized to evaluate the proposed neural network model. A sensitivity study of the involved parameters in the experimental work, i.e. pH, adsorbent dosage and initial concentration, was implemented. In addition, the adsorption rate order was investigated using three different kinetic models.

### Characterization of hybrid material

Studying the electric charge of any adsorbent is crucial due to its influence on the adsorption efficiency. The zeta potential is considered as the electrical potential between the bulk fluid and the surface across the dielectrical layer attached to the suspended particles in a solution. This potential is a source of balancing electrostatic forces that keep the micro- or nano-particles stable in suspension or emulsion. Herein, the absolute zeta potential has increased from 5.5 to −37.6 mV for P-CNTs and DK-CNTs respectively. In addition, the Raman spectra show that the $I_D/I_G$ (Intensity defect/Intensity graphite) ratio also increased from 1.11 for the P-CNTs to 1.2 for DK-CNTs indicating the presence of new functional groups in $sp^3$ direction resulting from the functionalization effect of D-DES. These functional groups play a significant role in increasing the adsorption capacity of DK-CNTs. FTIR results were in accordance with Raman results. The $sp^3$ direction functionalization was observed by OH stretching appearing in the peaks around 3,400 $cm^{-1}$. The N–H stretches were in the range of 3,207 $cm^{-1}$. In addition, the presence of C–Cl bonds may overlap with other CO groups between 600 and 700 $cm^{-1}$.

It is well known that the surface area of the adsorbent has a huge effect on the adsorption system. The introduction of D-DES as a functionalization agent of CNTs increased the

surface area significantly from 123.5 to 200.5 $m^2/g$. This significant increment is reflected in the maximum adsorption capacity of DK-CNTs (AlOmar *et al.* 2017). The functionalized CNTs showed a better result in the arsenic removal compared to the pristine CNT (AlOmar *et al.* 2016a).

## NARX modelling and performance

Selection of the right NARX network structure with good productivity and accuracy is a complicated task, which includes many points such as the selection of the proper number of hidden layers and the neurons number at the hidden layer. In general, the NARX network structure contains input layer(s), hidden layer(s) and output layer(s). The network selection has been carried out based on the network performance and productivity, using the MSE value during the training phase.

The parameters used in this work were arsenic concentration (1 to 5 mg/L), adsorbent dosage (20 to 40 mg), pH (3 to 8), and contact time until the equilibrium of reaction. One hundred and fifty-six (156) combinations were prepared in lab scale and divided into two sets (training set and testing set), 136 data were used for the training and 20 data were used for the testing. The MATLAB R2014a computational platform was used in the current study to code and optimize the network structure. The optimum hidden layers used for the model creation are two hidden layers with 10 neurons in each hidden layer with one input layer consisting of four nodes and one output layer with one node. The back-propagation training algorithm (*trainlm*) was selected to update the bias and weight vector values corresponding to the momentum, and the tangent sigmoid transfer function (*tansig*) was selected as the neuron transfer function for the network. The node numbers at the hidden layer were selected by training and testing the network using different neuron numbers and checking the value of the MSE of the testing set. The network performance depends on the net input, weight of trainlm and tangent sigmoid transfer function, tansig. The minimum value of MSE achieved was $4.75 \times 10^{-4}$ at the testing set, with correlation coefficient ($R^2$) of 0.9922, which shows a good agreement between the actual and the predicted data, the correlation coefficient plot for the testing set is presented in Figure 2. Different indicators were used to evaluate the trained model such as the relative

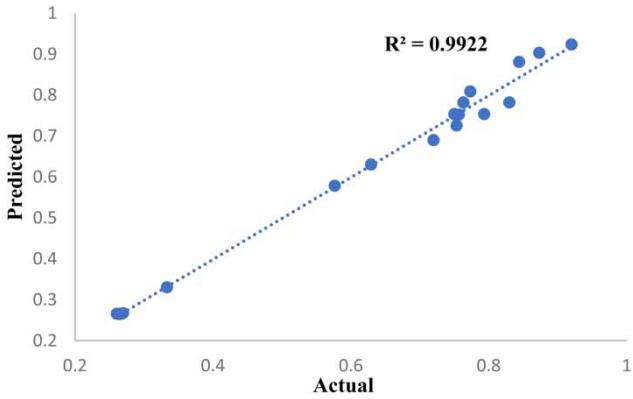


**Figure 2** | Correlation coefficient of actual and predicted normalized arsenic removal (testing dataset).

root mean square error (RRMSE), the root mean square error (RMSE), the mean square error (MSE) and mean absolute percentage error (MAPE). The results of all these indicators are presented in Table 1. The relative error is one of the indicators used in the modelling prediction and it compares the actual values to predicted values. Figure 3 shows the percentage relative error of the model. The maximum relative error value for the NARX model was 5.79%. The best prediction performance depends on the accuracy of the

**Table 1** | Evaluation indicators

| | NARX |
|---|---|
| MSE | $4.75 \times 10^{-4}$ |
| RMSE | $4.87 \times 10^{-3}$ |
| RRMSE | $2.78 \times 10^{-3}$ |
| MAPE | 2.05 |

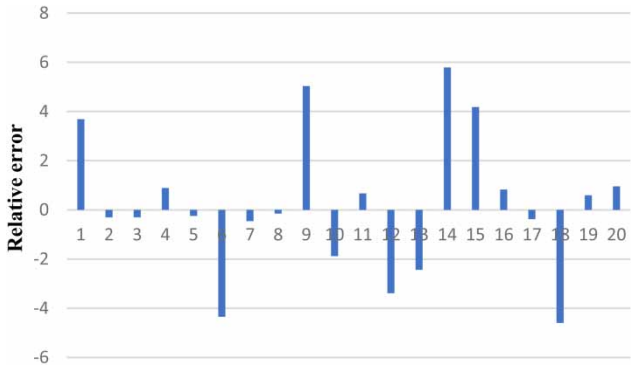


**Figure 3** | Illustration of the accuracy of the hybrid model based on the testing dataset.

neural network training. This study aimed to get the mathematical approach benefit during the real-time experiment. The NARX model development is becoming a challenge for the real-time experiment. The prepared NARX model used for the sensitivity study involved parameters in the experimental work (initial concentration, adsorbent dosage and pH). Moreover, the kinetic models were applied to the NARX outputs in order to check the model accuracy.

## Sensitivity study

### Initial concentration

The effect of initial concentration on the adsorption was studied by varying the $As^{3+}$ concentration from 1 to 5 mg/L, while all the other parameters such as pH (3), adsorbent dosage (20 mg) and contact time (5 min) were kept constant at their nominal levels indicated. The $As^{3+}$ adsorption percentage is inversely proportional to the $As^{3+}$ initial concentration. The adsorption capacity increases with increasing the initial metals concentration at a fixed adsorbent dosage. When the initial $As^{3+}$ concentration was increased from 1 to 3 mg/L, the adsorption capacity also increased from 2.18 to 3.56 mg/g. Whereas, in increasing the initial $As^{3+}$ concentration from 3 to 5 mg/L the adsorption capacity increased from 3.56 to 5.64 mg/g. This might be attributed to the increase in the driving force of the mass transfer which led to an increase in the uptake capacity of $As^{3+}$ ions from the water solution. At low concentration, the $As^{3+}$ ions interact with the adsorbent active sites. On the other hand, at higher $As^{3+}$ concentration, the adsorbent active sites are saturated and the removal percentage decreases (Banerjee *et al.* 2016). The obtained experimental data are used for training in the NARX modelling techniques. The NARX model prediction results were found to be in good agreement with the experimental data observation. The experimental and the NARX outputs are presented in Figure 4.

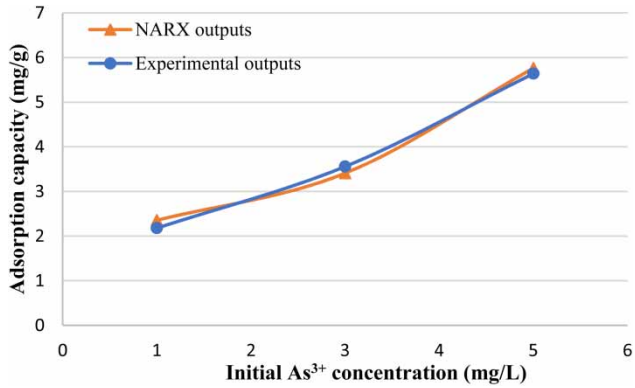


**Figure 4** | Experimental and NARX outputs as a function of initial concentration.

### pH effect

The aqueous solution pH is one of the most important parameters in controlling the adsorption and ion exchange. It is known that the pH can affect the functional groups (i.e. amino groups, phosphate and carboxyl) protonation in the biomass, and also the metal chemistry (i.e. its solubility) (Kazemipour *et al.* 2008; Witek-Krowiak *et al.* 2011). The effect of pH was examined by varying its value from 3 to 8, and fixing all the other involved parameters such as, adsorbent dosage (20 mg), initial concentration (1 mg/L) and contact time (50 min) at their nominal levels indicated.

It can be observed in Figure 5 that the adsorption capacity of DK-CNTs was increased with the increase of pH value until pH 6. Thereafter, the adsorption capacity became almost steady with increasing pH from 6 to 8. This increase may be due to the presence of the negative charge of the oxygen-containing functional groups, such as the carboxylic group, and the concentration of the negative electron charges enhanced by the presence of OH– in the solution. This pattern of negative charge intensive distribution on the surface of the adsorbent may be responsible for metal binding. It is well known that at pH greater than

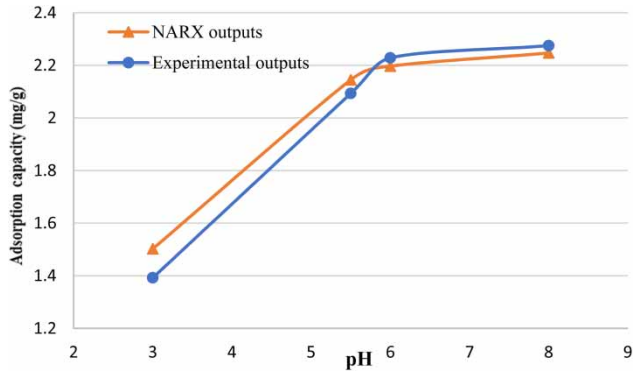


**Figure 5** | NARX outputs and experimental data as a function of pH.

7.0, the dominant species of $As^{3+}$ are As $(OH)^{+}$. This complexation may occur due to the extensive presence of $OH^{-}$ at this pH level resulting in a precipitation form, this phenomenon was also stated by (Gupta *et al.* 2011). In addition, the decreasing of $H^{+}$ plays a significant role in the mechanism of $As^{3+}$ adsorption due to the decrease of competition for the active sites of the adsorbent. The NARX technique was used for the modelling and prediction of the obtained data from the experimental work. The NARX-based ANN model prediction results showed good agreement with the experimental result trend. The NARX outputs and the experimental results as a function of pH versus the uptake capacity are presented in Figure 5.

### Adsorbent dosage study

The effect of adsorbent dosage was studied by varying the adsorbent dosage from 20 to 40 mg under a fixed time of 90 min, initial concentration of 3 mg/L and pH of 6. It can be seen from Figure 6 that the adsorption capacity of $As^{3+}$ ions decreased with increasing the DK-CNTs adsorbent dosage value. The adsorption capacity for 20 mg dosage was 7.56 mg/g then, as the DK-CNTs adsorbent was increased to 30 and 40 mg the adsorption capacity decreased to 6.23 and 5.89 mg/g, respectively. The decrease in the arsenic uptake capacity as the adsorbent dosage increases might be attributed to the increase of more active sites due to the addition of adsorbent surface area which was also reported by Das *et al.* (2014). The obtained experimental data were used in training and prediction by using the NARX modelling techniques. The NARX model prediction was found to be satisfactory for the experimental data observation. The experimental and predicted outputs of the NARX are presented in Figure 6.

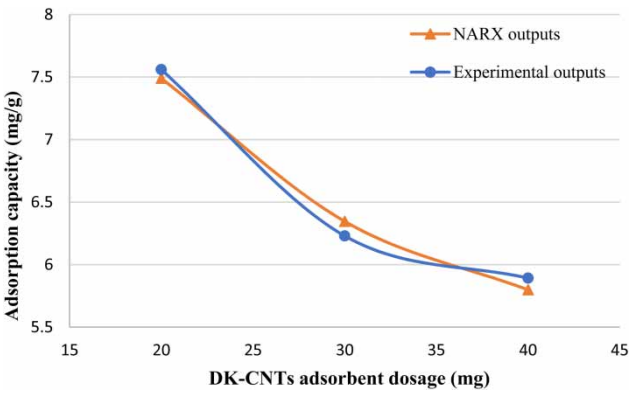


**Figure 6** | Experimental and NARX outputs as a function of adsorbent dosage.

### Adsorption kinetics study

Three adsorption kinetic models were implemented in this study to investigate the $As^{3+}$ adsorption rate and mechanism as well as the solute removal rate (Ayoob *et al.* 2007). The intraparticle diffusion, pseudo-first-order and pseudo-second-order models were used in this work. The kinetic studies were achieved at different pH values (3, 5.5 and 8) and initial concentration (1 and 3 mg/L) with different adsorbent dosage (20 and 30 mg) and agitation speed of 180 rpm. The correlation coefficient ($R^2$) was used as the conformity indicator of the kinetic models between the experiment and the predicted adsorption values for each kinetic model. The pseudo-second-order model best described the adsorption kinetics of the system and the results are presented in Figure 7, as time over adsorption capacity ($T/Q$). The results of the intraparticle diffusion and pseudo-first-order models are presented in Table 2. The kinetics study results reveal that the amount of DK-CNTs adsorbent and its concentration are associated with the rate determination step, which indicates that the rate limiting step involves chemisorption. The same behaviour was reported elsewhere (Veličković *et al.* 2013).

The NARX neural network technique was used for modelling and prediction of the obtained data from the experimental work. The three kinetics models used for modelling the experimental data were also applied on the NARX outputs. The pseudo-second-order model best described the adsorption kinetics of this study as compared to the intraparticle diffusion and pseudo-first-order models. The results of the kinetics study are presented in Table 2. The NARX model shows good agreement with the experimental work, which shows that the NARX model has high accuracy.

## CONCLUSION

A new adsorbent was developed using a DES system as the functionalization agent of carbon nanotubes. The amount of

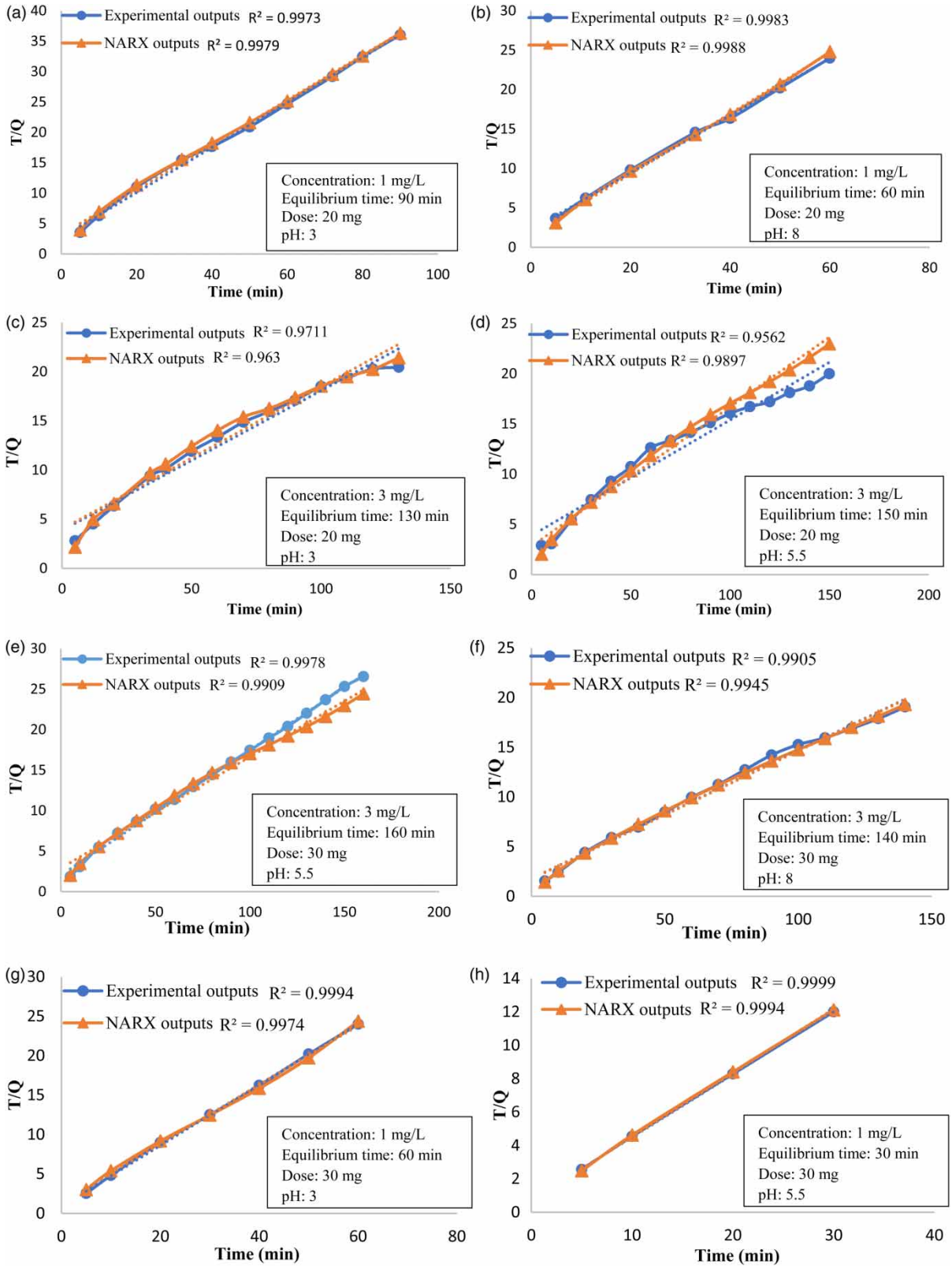


**Figure 7** | Kinetics study.

**Table 2** | Adsorption kinetics and correlation coefficient

| | | | Pseudo-first-order $ln\ (q_e-q_t)$ vs time (t) | | Pseudo-second-order $(t/q_t$ vs t) | | Intraparticle $(q_t$ vs $t^{0.5})$ | |
|---|---|---|---|---|---|---|---|---|
| Dose mg | PH | $C_0$ mg/L | Experimental $R^2$ | NARX output $R^2$ | Experimental $R^2$ | NARX outputs $R^2$ | Experimental $R^2$ | NARX outputs $R^2$ |
| 20 | 3 | 1 | 0.8925 | 0.9052 | 0.9973 | 0.9979 | 0.7471 | 0.7172 |
| 20 | 8 | 1 | 0.5483 | 0.5997 | 0.9983 | 0.9988 | 0.6496 | 0.6244 |
| 20 | 3 | 3 | 0.656 | 0.6819 | 0.9711 | 0.963 | 0.7931 | 0.7311 |
| 20 | 5.5 | 3 | 0.7858 | 0.7017 | 0.9562 | 0.9897 | 0.6775 | 0.6884 |
| 30 | 5.5 | 3 | 0.8939 | 0.8682 | 0.9978 | 0.9909 | 0.5338 | 0.5848 |
| 30 | 8 | 3 | 0.6758 | 0.6069 | 0.9905 | 0.9945 | 0.7542 | 0.795 |
| 30 | 3 | 1 | 0.756 | 0.7888 | 0.9994 | 0.9974 | 0.5921 | 0.5229 |
| 30 | 5.5 | 1 | 0.8102 | 0.8608 | 0.9999 | 0.9994 | 0.674 | 0.6838 |

arsenic removal increased with the increasing of contact time, pH and initial concentration, whereas the arsenic removal decreased with increasing adsorbent dosage. Comparing the experiment results with the NARX model outputs, it can be concluded that the NARX model is able to predict the amount of arsenic removal from water sufficiently with acceptable error. The minimum value of MSE achieved was $4.75 \times 10^{-4}$ at the testing set, with correlation coefficient ($R^2$) of (0.9922), which shows a good agreement between the actual and the predicted data. Other indicators were also used such as the RMSE ($4.87 \times 10^{-3}$), RRMSE ($2.78 \times 10^{-3}$) and MAPE (2.05). All these indicators confirmed the high accuracy of the NARX model.

## ACKNOWLEDGEMENTS

The authors express their thanks to the University of Malaya for funding this research. UMRG (RP044D-17AET) and (RP025A-18SUS).

## REFERENCES

Abbott, A. P., Boothby, D., Capper, G., Davies, D. L. & Rasheed, R. K. 2004 Deep eutectic solvents formed between choline chloride and carboxylic acids: versatile alternatives to ionic liquids. *Journal of the American Chemical Society* **126** (29), 9142–9147.

Abbott, A. P., Capper, G., McKenzie, K. J. & Ryder, K. S. 2007 Electrodeposition of zinc–tin alloys from deep eutectic solvents based on choline chloride. *Journal of Electroanalytical Chemistry* **599** (2), 288–294.

Abbott, A. P., Griffith, J., Nandhra, S., O'Connor, C., Postlethwaite, S., Ryder, K. S. & Smith, E. L. 2008 Sustained electroless deposition of metallic silver from a choline chloride-based ionic liquid. *Surface and Coatings Technology* **202** (10), 2033–2039.

Abo-Hamad, A., Hayyan, M., AlSaadi, M. A. & Hashim, M. A. 2015 Potential applications of deep eutectic solvents in nanotechnology. *Chemical Engineering Journal* **273**, 551–567.

Agami, N., Atiya, A., Saleh, M. & El-Shishiny, H. 2009 A neural network based dynamic forecasting model for Trend Impact Analysis. *Technological Forecasting and Social Change* **76** (7), 952–962.

Ahmadi, Y., Eshraghi, S. E., Bahrami, P., Hasanbeygi, M., Kazemzadeh, Y. & Vahedian, A. 2015 Comprehensive Water–Alternating-Gas (WAG) injection study to evaluate the most effective method based on heavy oil recovery and asphaltene precipitation tests. *Journal of Petroleum Science and Engineering* **133**, 123–129.

Ali, I. 2012 New generation adsorbents for water treatment. *Chemical Reviews* **112** (10), 5073–5091.

AlOmar, M. K., Alsaadi, M. A., Hayyan, M., Akib, S. & Hashim, M. A. 2016a Functionalization of CNTs surface with phosphonium based deep eutectic solvents for arsenic removal from water. *Applied Surface Science* **389**, 216–226.

AlOmar, M. K., Hayyan, M., Alsaadi, M. A., Akib, S., Hayyan, A. & Hashim, M. A. 2016b Glycerol-based deep eutectic solvents: physical properties. *Journal of Molecular Liquids* **215**, 98–103.

AlOmar, M. K., Alsaadi, M. A., Aljumaily, M. M., Akib, S., Jassam, T. M. & Hashim, M. A. 2017 N, N-Diethylethanolammonium chloride-based DES-functionalized carbon nanotubes for arsenic removal from aqueous solution. *Desalination and Water Treatment* **74**, 163–173.

Argos, M., Kalra, T., Rathouz, P. J., Chen, Y., Pierce, B., Parvez, F., Islam, T., Ahmed, A., Rakibuz-Zaman, M. & Hasan, R. 2010

Arsenic exposure from drinking water, and all-cause and chronic-disease mortalities in Bangladesh (HEALS): a prospective cohort study. *The Lancet* **376** (9737), 252–258.

Atieh, M. A., Bakather, O. Y., Al-Tawbini, B., Bukhari, A. A., Abuilaiwi, F. A. & Fettouhi, M. B. 2011 Effect of carboxylic functional group functionalized on carbon nanotubes surface on the removal of lead from water. *Bioinorganic Chemistry and Applications*. doi:10.1155/2010/603978.

Ayoob, S., Gupta, A. & Bhakat, P. 2007 Performance evaluation of modified calcined bauxite in the sorptive removal of arsenic (III) from aqueous environment. *Colloids and Surfaces A: Physicochemical and Engineering Aspects* **293** (1), 247–254.

Banerjee, A., Sarkar, P. & Banerjee, S. 2016 Application of statistical design of experiments for optimization of As (V) biosorption by immobilized bacterial biomass. *Ecological Engineering* **86**, 13–23.

Chen, J. P. & Wu, S. 2004 Acid/base-treated activated carbons: characterization of functional groups and metal adsorptive properties. *Langmuir* **20** (6), 2233–2242.

Chen, S., Billings, S. & Grant, P. 1990 Non-linear system identification using neural networks. *International Journal of Control* **51** (6), 1191–1214.

Cho, D.-W., Song, H., Kim, B., Schwartz, F. W. & Jeon, B.-H. 2015 Reduction of nitrate in groundwater by Fe (0)/Magnetite nanoparticles entrapped in Ca-Alginate beads. *Water, Air, & Soil Pollution* **226** (7), 206.

Cooper, E. R., Andrews, C. D., Wheatley, P. S., Webb, P. B., Wormald, P. & Morris, R. E. 2004 Ionic liquids and eutectic mixtures as solvent and template in synthesis of zeolite analogues. *Nature* **430** (7003), 1012–1016.

Çoruh, S., Geyikçi, F., Kılıç, E. & Çoruh, U. 2014 The use of NARX neural network for modeling of adsorption of zinc ions using activated almond shell as a potential biosorbent. *Bioresource Technology* **151**, 406–410.

Das, B., Mondal, N., Bhaumik, R. & Roy, P. 2014 Insight into adsorption equilibrium, kinetics and thermodynamics of lead onto alluvial soil. *International Journal of Environmental Science and Technology* **11** (4), 1101–1114.

Ding, Z., Hu, X., Morales, V. L. & Gao, B. 2014 Filtration and transport of heavy metals in graphene oxide enabled sand columns. *Chemical Engineering Journal* **257**, 248–252.

Fayaed, S. S., El-Shafie, A. & Jaafar, O. 2013 Adaptive neuro-fuzzy inference system-based model for elevation–surface area–storage interrelationships. *Neural Computing and Applications* **22** (5), 987–998.

Fiyadh, S. S., AlSaadi, M. A., AlOmar, M. K., Fayaed, S. S., Hama, A. R., Bee, S. & El-Shafie, A. 2017 The modelling of lead removal from water by deep eutectic solvents functionalized CNTs: artificial neural network (ANN) approach. *Water Science and Technology* **76** (9), 2413–2426.

Gorke, J. T., Srienc, F. & Kazlauskas, R. J. 2008 Hydrolase-catalyzed biotransformations in deep eutectic solvents. *Chemical Communications* **10**, 1235–1237.

Gupta, V., Rastogi, A., Saini, V. & Jain, N. 2006 Biosorption of copper (II) from aqueous solutions by Spirogyra species. *Journal of Colloid and Interface Science* **296** (1), 59–63.

Gupta, V. K., Agarwal, S. & Saleh, T. A. 2011 Synthesis and characterization of alumina-coated carbon nanotubes and their application for lead removal. *Journal of Hazardous Materials* **185** (1), 17–23.

Hayyan, M., Abo-Hamad, A., AlSaadi, M. A. & Hashim, M. A. 2015 Functionalization of graphene using deep eutectic solvents. *Nanoscale Research Letters* **10** (1), 324.

Hu, S., Shi, Q. & Jing, C. 2015 Groundwater arsenic adsorption on granular $TiO_2$: integrating atomic structure, filtration, and health impact. *Environmental Science & Technology* **49** (16), 9707–9713.

Kamble, S. P., Jagtap, S., Labhsetwar, N. K., Thakare, D., Godfrey, S., Devotta, S. & Rayalu, S. S. 2007 Defluoridation of drinking water using chitin, chitosan and lanthanum-modified chitosan. *Chemical Engineering Journal* **129** (1), 173–180.

Kazemipour, M., Ansari, M., Tajrobehkar, S., Majdzadeh, M. & Kermani, H. R. 2008 Removal of lead, cadmium, zinc, and copper from industrial wastewater by carbon developed from walnut, hazelnut, almond, pistachio shell, and apricot stone. *Journal of Hazardous Materials* **150** (2), 322–327.

Kocabaş-Ataklı, Z. Ö. & Yürüm, Y. 2013 Synthesis and characterization of anatase nanoadsorbent and application in removal of lead, copper and arsenic from water. *Chemical Engineering Journal* **225**, 625–635.

Leroy, E., Decaen, P., Jacquet, P., Coativy, G., Pontoire, B., Reguerre, A.-L. & Lourdin, D. 2012 Deep eutectic solvents as functional additives for starch based plastics. *Green Chemistry* **14** (11), 3063–3066.

Lourie, E. & Gjengedal, E. 2011 Metal sorption by peat and algae treated peat: kinetics and factors affecting the process. *Chemosphere* **85** (5), 759–764.

Luo, X., Zhang, Z., Zhou, P., Liu, Y., Ma, G. & Lei, Z. 2015 Synergic adsorption of acid blue 80 and heavy metal ions (Cu 2 + /Ni 2+) onto activated carbon and its mechanisms. *Journal of Industrial and Engineering Chemistry* **27**, 164–174.

Martinez, M., Callejas, M., Benito, A., Cochet, M., Seeger, T., Anson, A., Schreiber, J., Gordon, C., Marhic, C. & Chauvet, O. 2003 Modifications of single-wall carbon nanotubes upon oxidative purification treatments. *Nanotechnology* **14** (7), 691.

Mazumder, D. G., Mandal, B., Chowdhury, T., Samanta, G., Basu, G., Chowdhury, P., Chanda, C., Lodh, D. & Chakraborti, D. 1997 Chronic arsenic toxicity in West Bengal. *Current Science* **72** (1), 114–117.

McAvoy, T. J. & Werbos, P. 1992 Long-term predictions of chemical processes using recurrent neural networks: a parallel training approach. *Industrial & Engineering Chemistry Research* **31** (5), 1338–1352.

Oubagaranadin, J. U. K. & Murthy, Z. 2010 Isotherm modeling and batch adsorber design for the adsorption of Cu (II) on a clay

containing montmorillonite. *Applied Clay Science* **50** (3), 409–413.

Paiva, A., Craveiro, R., Aroso, I., Martins, M., Reis, R. L. & Duarte, A. R. C. 2014 Natural deep eutectic solvents – solvents for the 21st century. *ACS Sustainable Chemistry & Engineering* **2** (5), 1063–1071.

Ramos, M. L. P., González, J. A., Albornoz, S. G., Pérez, C. J., Villanueva, M. E., Giorgieri, S. A. & Copello, G. J. 2016 Chitin hydrogel reinforced with $TiO_2$ nanoparticles as an arsenic sorbent. *Chemical Engineering Journal* **285**, 581–587.

Rao, G. P., Lu, C. & Su, F. 2007 Sorption of divalent metal ions from aqueous solution by carbon nanotubes: a review. *Separation and Purification Technology* **58** (1), 224–231.

Smith, A. H., Lopipero, P. A., Bates, M. N. & Steinmaus, C. M. 2002 Arsenic epidemiology and drinking water standards. *Science* **296** (5576), 2145–2146.

Sun, Y.-P., Fu, K., Lin, Y. & Huang, W. 2002 Functionalized carbon nanotubes: properties and applications. *Accounts of Chemical Research* **35** (12), 1096–1104.

Thostenson, E. T., Ren, Z. & Chou, T.-W. 2001 Advances in the science and technology of carbon nanotubes and their composites: a review. *Composites Science and Technology* **61** (13), 1899–1912.

Veličković, Z. S., Marinković, A. D., Bajić, Z. J., Marković, J. M., Perić-Grujić, A. A., Uskokovic, P. S. & Ristic, M. D. 2013 Oxidized and ethylenediamine-functionalized multi-walled carbon nanotubes for the separation of low concentration arsenate from water. *Separation Science and Technology* **48** (13), 2047–2058.

Wang, S.-X., Wang, Z.-H., Cheng, X.-T., Li, J., Sang, Z.-P., Zhang, X.-D., Han, L.-L., Qiao, X.-Y., Wu, Z.-M. & Wang, Z.-Q. 2007 Arsenic and fluoride exposure in drinking water: children's IQ and growth in Shanyin county, Shanxi province, China. *Environmental Health Perspectives* **115** (4), 643–647.

Wasserman, G. A., Liu, X., Parvez, F., Ahsan, H., Factor-Litvak, P., van Geen, A., Slavkovich, V., Lolacono, N. J., Cheng, Z. & Hussain, I. 2004 Water arsenic exposure and children's intellectual function in Araihazar, Bangladesh. *Environmental Health Perspectives* **112** (13), 1329–1333.

Witek-Krowiak, A., Szafran, R. G. & Modelski, S. 2011 Biosorption of heavy metals from aqueous solutions onto peanut shell as a low-cost biosorbent. *Desalination* **265** (1), 126–134.

Xia, S., Shen, S., Xu, X., Liang, J. & Zhou, L. 2014 Arsenic removal from groundwater by acclimated sludge under autohydrogenotrophic conditions. *Journal of Environmental Sciences* **26** (2), 248–255.

Xu, K., Wang, Y., Huang, Y., Li, N. & Wen, Q. 2015 A green deep eutectic solvent-based aqueous two-phase system for protein extracting. *Analytica Chimica Acta* **864**, 9–20.

Zhang, Q., Vigier, K. D. O., Royer, S. & Jérôme, F. 2012 Deep eutectic solvents: syntheses, properties and applications. *Chemical Society Reviews* **41** (21), 7108–7146.

First received 28 June 2017; accepted in revised form 2 July 2018. Available online 20 July 2018